Bioorganic & Medicinal Chemistry 26 (2018) 4088–4099

Contents lists available at ScienceDirect

Bioorganic & Medicinal Chemistry

journal homepage: www.elsevier.com/locate/bmc

Identification of natural product compounds as quorum sensing inhibitors in *Pseudomonas fluorescens* P07 through virtual screening

Ting Ding[a], Tingting Li[b], Jianrong Li[a,c,*]

[a] School of Food Science and Technology, Jiangnan University, Wuxi 214122, China
[b] Key Laboratory of Biotechnology and Bioresources Utilization (Dalian Minzu University), Ministry of Education, Dalian, Liaoning 116600, China
[c] College of Food Science and Technology, Bohai University; Food Safety Key Lab of Liaoning Province; National & Local Joint Engineering Research Center of Storage, Processing and Safety Control Technology for Fresh Agricultural and Aquatic Products, Jinzhou, Liaoning 121013, China

ARTICLE INFO

InChIKeys:
WVDDGKGOMKODPV-UHFFFAOYSA-N
QMVPMAAFGQKVCJ-JTQLQIEISA-N
GSFBRCUXDDCNKV-UHFFFAOYSA-N
DPGLBHQUHFJRJS-RQOWECAXSA-N
QBDCOUHKEVYWLO-UHFFFAOYSA-N
VMBKZHMLQXCNCP-NSHDSACASA-N
Keywords:
Pseudomonas fluorescens P07
Quorum sensing
Biofilm formation
Virtual screening
Molecular docking
Whole-genome sequencing

ABSTRACT

Pseudomonas fluorescens, a Gram-negative psychrotrophic bacteria, is the main microorganism causing spoilage of chilled raw milk and aquatic products. Quorum sensing (QS) widely exists in bacteria to monitor their population densities and regulate numerous physiological activities, such as the secretion of siderophores, swarming motility and biofilm formation. Thus, searching for quorum sensing inhibitors (QSIs) may be another promising way to control the deterioration of food caused by *P. fluorescens*. Here, we screened a traditional Chinese medicine (TCM) database to discover potential QSIs with lesser toxicity. The gene sequences of LuxI- and LuxR-type proteins of *P. fluorescens* P07 were obtained through whole-genome sequencing. In addition, the protein structures built by homology modelling were used as targets to screen for QSIs. Twenty-one compounds with a dock score greater than 6 were purchased and tested by biosensor strains (*Chromobacterium violaceum* CV026 and *Agrobacterium tumefaciens* A136). The results showed that 10 of the compounds were determined as hits (hit rate: 66.67%). Benzyl alcohol, rhodinyl formate and houttuynine were effective QSIs. The impact of the most active compound (benzyl alcohol) on the phenotypes of *P. fluorescens* P07, including swimming and swarming motility, production of extracellular enzymes and siderophores, *N*-acylhomoserine lactone (AHLs) content and biofilm formation were determined. The inhibitory mechanism of benzyl alcohol on the QS system of *P. fluorescens* P07 is further discussed. This study reveals the feasibility of searching for novel QSIs through virtual screening.

1. Introduction

Pseudomonas fluorescens is a type of rod-shaped, motile, gram-negative and food-borne pathogenic bacterium.[1] It has been recognized as the main spoiler and contaminant in refrigerated foods, such as aquatic products, milk, beef and meat, since the organisms grow well even at low temperatures.[2–5] *P. fluorescens* can produce heat-tolerant proteases and lipases, which is one of the main reasons for the rancid flavours and odours that finally make the foods unacceptable to consumers and lead to the loss of food quality.[6–8] With the increasing customer demands for high-quality and safe refrigerated food, it is important to control the food spoilage caused by *P. fluorescens*.

Many bacteria use signalling molecules, namely, autoinducers (AIs), to communicate. This mechanism was called quorum sensing (QS).[2,9–11] AIs accumulate with the increase of quorum sensing bacterial cells. Detection of AIs by bacteria will stimulate the expression of corresponding genes once the threshold is reached.[12–14] AHLs are used by most gram-negative bacteria.[15–17] Numerous bacterial physiological activities are controlled by quorum sensing, such as biofilm formation, surface colonization, swimming and swarming motility, bioluminescence, cell differentiation, competence, symbiosis, conjugation, sporulation, and production of siderophores, pigments, toxins, enzymes and antibiotics.[18–21] Hence, a promising strategy to control food spoilage may be to target bacterial QS system.

The discovery of quorum sensing inhibitors (QSIs) has been intensively investigated in recent years. Various substances have been identified as QSIs, such as vanilla extract,[22] quercetin,[15] polyphenolic extract,[23] aspirin[17] and curcumin.[24] However, traditional ways of finding QSIs are expensive, time-consuming, random and inefficient. Virtual screening (VS) can be used to solve this problem. A wide variety of useful compounds that exhibit desired biological activities were identified through computational methods in VS. Lin et al. screened promising human HMG-CoA reductase (hHMGR) inhibitors from natural products by using a virtual screening method in order to find

* Corresponding author at: College of Food Science and Technology, Bohai University, Jinzhou, Liaoning, China.
E-mail address: 13804242235@163.com (J. Li).

https://doi.org/10.1016/j.bmc.2018.06.039
Received 26 April 2018; Received in revised form 17 June 2018; Accepted 28 June 2018
Available online 30 June 2018
0968-0896/

hypolipidemic drug candidates. They found that curcumin and salvianolic acid C had the ability to significantly inhibit hHMGR. The results revealed that searching for novel drug candidates *via* VS is feasible.[25] Similarly, Sommer and co-workers discovered novel compounds that may modulate dopamine D2 receptor (D2R) pathways from bioactive food components by using the VS method. They found that hordenine had approximately the same effectiveness as dopamine (76%) and significantly contributed to the mood-elevating effects of beer.[26]

Traditional Chinese medicines (TCMs) have been used for thousands of years in China. They have been widely used to combat various ailments with fewer side effects and higher efficiency.[20,27–30] A wide range of bioactive compounds from TCMs have been identified to treat various diseases, while there is almost no literature about the applications of virtual screening for QSIs from TCMs in food-borne bacteria. Hence, in this study, we virtually screened the potential QSIs of *P. fluorescens* P07 from a TCM database. The anti-QS mechanism of benzyl alcohol is further discussed.

2. Materials and methods

All standard AHLs (C4-HSL, C6-HSL, C8-HSL, C10-HSL, C12-HSL and C14-HSL) and X-Gal (5-bromo-4-chloro-3-indoyl-β-d-galactopyranoside) were obtained from Sigma-Aldrich (St. Louis, MO, USA). AHLs were prepared at a 20 μM concentration (dissolved in methanol). X-Gal was prepared at a 20 mg/ml concentration. Luria-Bertani (LB) medium was purchased from Beijing Aoboxing Biotech Company. *C. violaceum* CV026 and *A. tumefaciens* A136 were used as indicator strains. As a mini-Tn5 mutant, *C. violaceum* CV026 is unable to produce AHLs, but it secretes purple violacein when it encounters exogenous short chain AHLs (mainly C6-HSL).[31] The *lacZ* gene is expressed in *A. tumefaciens* A136, where exogenous long chain AHLs (mainly C10-HSL) and X-Gal exist, leading to the secretion of β-galactosidase and, thus, eventually to the blue colour of the plates. *P. fluorescens* P07 was isolated from deteriorated turbot (*Scophthalmus maximus*) and was identified and stored at −80 °C in our laboratory. All the strains were diluted 1:100 in 10 ml of LB medium with shaking (160 rpm) at 28 °C to an OD_{600} of 1.0. In particular, the two indicator strains were additionally supplemented with 20 μg/ml of tetracycline (10 μl), 20 μg/ml of spectinomycin (50 μl) and 20 μg/ml of kanamycin (10 μl), respectively. All chemicals were commercially available.

2.1. Whole-genome sequencing of P. fluorescens P07

2.1.1. Genome sequencing and assembly

P. fluorescens P07 was diluted 1:100 in 100 ml of LB medium and cultured overnight with shaking (160 rpm) at 28 °C. The DNA was extracted according to the bacterial genome DNA isolation kit. Agarose gel electrophoresis was applied to detect the harvested DNA and quantified by Qubit. Agilent 2100 was used to detect the size of the inserted fragments, and then sequenced by PacBio RSII platform. Single molecule, real-time (SMRT) technology was used to sequence the genome of *P. fluorescens* P07 at the Beijing Novogene Bioinformatics Technology Co., Ltd. SMRT 2.3.0 was used to filter the low quality reads,[32,33] and finally, one contig without gaps was generated after the filtered reads were assembled.

2.1.2. Genome component prediction

Genome component prediction included the prediction of the coding gene, repetitive sequences, non-coding RNA, genomics islands, transposon, *etc*. The programs are listed in Table S1 (Supplemental material S1).

2.1.3. Gene function

Seven databases were used to predict gene functions: Gene Ontology (GO),[34] Kyoto Encyclopedia of Genes and Genomes (KEGG),[35,36] Clusters of Orthologous Groups (COG),[37] Non-Redundant Protein Database (NR),[38] Transporter Classification Database (TCDB),[39] Swiss-Prot[40] and TrEMBL.[41] A whole genome Blast[42] search was carried out against the above databases (E-value < 1e-5, minimal alignment length percentage > 40%). The SignalP[43] database was used to predict the secretory proteins, and the prediction of Type I-VII proteins secreted by the pathogenic bacteria was based on the EffectiveT3 software.[44]

2.2. Homology modelling

The amino acids sequences of acyl-homoserine-lactone synthase (LuxI-type protein) and LuxR family transcriptional regulators (LuxR-type protein) were obtained through whole-genome sequencing. The sequences were submitted to SWISS-MODEL (https://swissmodel.expasy.org) to construct 3D structure of proteins.[45] The most homologous sequences (identity > 30%) of the two proteins of *P. fluorescens* P07 were selected as templates for homology modelling. In addition, the best models were selected from the top-ranked 50 models.

2.3. Model evaluation

The LuxI- and LuxR-type proteins of *P. fluorescens* P07 constructed by SWISS-MODEL were evaluated by RAMPAGE[46] (http://mordred.bioc.cam.ac.uk/~rapper/rampage.php) and the QMEAN method (https://swissmodel.expasy.org/qmean/).

2.4. Virtual screening and molecular docking

Energy minimization of the built protein models was performed by the SYBYL-X 2.1 program (Triops, Triops, Inc., USA) and included adding hydrogen atoms, removing water molecules, and repairing side chains for molecular docking. The 3D structure of the compounds from the TCM database (http://ibts.hkbu.edu.hk/LSP/index.php) were optimized by a standard Tripos molecular mechanics force field (convergence criterion: 0.005 kcal/(Å mol)). Compounds whose molecular weights were lower than 500 were selected (10354 molecules). Partial atomic charges were calculated by Gasteiger-Hückel. Selected compounds were optimized and docked with the respective prepared proteins by the Surflex-Dock program in SYBYL-X 2.1 (Protomol generation mode: automatic; docking mode: Surflex-Dock screen (SFXC); other docking process was performed according to default settings). Furanone C-30 which has been identified to be inhibitors of QS system was taken as control to be docked with LuxI- and LuxR-type proteins of *P. fluorescens* P07.[47] The compounds with high docking scores (Total Score > 6 and CScore > 4) were selected and purchased to identify whether they had quorum sensing inhibitory activities.

2.5. AHLs extraction

An overnight culture of *P. fluorescens* P07 (2 ml) was added to 200 ml of LB medium and cultured to an OD_{600} of 1.0 (160 rpm, 28 °C). Then, the culture was centrifuged at 12,000*g* for 4 min, after which the cells were discarded. The AHLs were extracted with 200 ml of ethyl acetate (contained 0.1% acetic acid (v/v)) twice and were left standing for one hour. The extract was rotary evaporated at 35 °C, and then 1 ml of methanol was added and stored at −20 °C.

2.6. AHL detection

C. violaceum CV026 and *A. tumefaciens* A136 served as indicator bacteria for AHL detection. The two strains (1 ml each) were routinely cultured and separately added to 100 ml of LB agar. The LB agar for *A. tumefaciens* A136 was supplemented with 100 μl of X-Gal. The extracted AHLs were streaked onto the congealed agar. The plates were incubated for 24 h at 28 °C. In particular, the plates for *A. tumefaciens* A136 were placed away from light because the X-Gal was easily decomposed.

2.7. MIC (minimum inhibitory concentration) determination of the selected compounds

The MICs of the selected compounds after virtual screening against indicator strains and *P. fluorescens* P07 were measured using the previously described method.[48] This step was determined to confirm that the QS inhibitory activities involved interfering with the QS system rather than preventing bacterial growth. The solid compounds were prepared to make 10 mg/ml of a stock solution. Rosmarinic acid and 1,10-decanediol were dissolved in sterile water and 70% methanol, respectively. In addition, undecanoic acid, 1-dodecanol, azelaic acid and houttuynine were dissolved in 60% dimethyl sulfoxide (DMSO). Rhodinyl formate and (−)-beta-citronellol were diluted in 60% DMSO. Furthermore, 70% methanol and 60% DMSO were used as blank controls. The compounds under sub-MIC were used in QS inhibition assays.

2.8. QS inhibitory assay

The QS inhibitory activities of the selected compounds were tested by indicator strains according to the Issac method.[21] The two indicator strains were routinely cultured, diluted 1:100 in 100 ml of LB agar and mixed thoroughly. For *C. violaceum* CV026, the LB medium was supplemented with 10 µl C6-HSL. For *A. tumefaciens* A136, 10 µl C10-HSL and 100 µl X-Gal were added to the LB medium. The prepared compounds (100 µl) were injected into the holes (6 mm) in the agar plates, and subsequently, the plates were placed in an incubator for 24 h at 28 °C. The colour change was observed in the plates. Hit rate was calculated as follows:

Hit rate = Compound showed anti-QS activities/All tested compounds.

2.9. Impact of benzyl alcohol on the QS-regulated phenotypes of P. fluorescens P07

Two millilitres of the overnight culture of *P. fluorescens* P07 (1.0 OD at 600 nm) were added to four Erlenmeyer flasks containing 200 ml of LB medium (as control) or 200 ml of LB medium supplemented with 0.05%, 0.10%, and 0.15% (v/v) benzyl alcohol, respectively. The Erlenmeyer flasks were incubated with 160 rpm agitation for 24 h at 28 °C. The overnight culture without benzyl alcohol was taken as the control. Then, the impact of benzyl alcohol on the QS-regulated phenotypes (including swimming and swarming motility; production of siderophores, AHLs and extracellular proteases; biofilm formation; and extracellular polymeric substances (EPSs) of *P. fluorescens* P07) were performed according to our previous methods.[48] Each measurement was performed in triplicate.

2.10. Raman spectrum test

The overnight culture (20 µl) of *P. fluorescens* P07 (1.0 OD at 600 nm) was added to four Petri dishes containing 20 ml of LB medium or 20 ml of LB medium supplemented with 0.05%, 0.10% and 0.15% (v/v) of benzyl alcohol, respectively. There was a slice of polished zinc (0.5 cm × 0.5 cm × 0.02 cm) in each Petri dish, and the zinc immersed in the LB medium without bacteria was served as a blank control. Then, the Petri dishes were placed in an incubator statically for 48 h (28 °C) to allow adherence of the biofilm onto the zinc. Next, the unattached bacteria on the zinc were removed with sterile PBS. The zinc was air dried for 30 min for a Raman spectrum test (wavelength of laser light source: 532 nm; power of the laser light source: 25 mW; 50× objective lens; exposure time: 20 s; exposure times: 5; spectrum range: 100–3500 cm^{-1}). Six random positions of the biofilm were chosen to perform the spectrum test.

2.11. Inhibition mechanism of benzyl alcohol

The inhibition mechanism of benzyl alcohol on the QS was analysed by Discovery Studio 4.5 Client (Accelrys Software, Inc., San Diego, CA, USA). Ligand-protein interactions were shown in both three-dimensional and two-dimensional plots. In order to clarify the inhibitory mechanism, benzyl alcohol and other compounds (ethyl linalool, rhodinyl formate, houttuynine and (−)-beta-citronellol) were docked with LuxI-type protein and the ligand-protein interactions were analysed. Besides, benzyl alcohol was also docked with LuxR-type protein and the known LuxI-type protein (LasI, PDB: 1ro5).

2.12. Statistical analysis

All the tests were repeated three times. The results are expressed as the means ± standard deviation (SD) and were analysed through one-way ANOVA by SPSS Statistics 16.0 (SPSS, Inc.) Significant differences are displayed at $p < 0.05$.

3. Results

3.1. Whole genome sequencing results

General and specific genome features of *P. fluorescens* P07 are presented in Table S2 (Supplemental material S2).

Whole genome sequencing of *P. fluorescens* P07 was completed by PacBio RSII (Pacific Biosciences, USA). Approximately 1,030,009,628 bp of data were produced, and 93,810 reads were used to assemble the draft genome of *P. fluorescens* P07 by SMRT portal software. *P. fluorescens* P07 harbours a circular chromosome of 6,030,570 bp, and its G/C content is 60.67% according to the genome. Genes were predicted by GeneMarkS (Version 4.17). Approximately 5515 genes and 99 non-coding RNAs (including 66 of tRNA, 6 of 5srRNA, 5 of 16SrRNA, 5 of 23SrRNA and 17of sRNA) were predicted from this assembly. The predicted coding sequences (CDSs) were searched against the COG, Go, KEGG, NR, Pfam, Swiss-Prot, TCDB and TnSS databases for annotation. These data sources were combined to obtain a product description for each predicted protein (Fig. S1) (Supplemental material S3), and the amino acid sequence of LuxI and LuxR type proteins of *P. fluorescens* P07 were obtained as follows:

The amino acid sequence of acyl-homoserine-lactone synthase (LuxI type):

> P07GM002262 locus = Chr1:2545087:2545665:- MISIITRHHHELSAALEDDLGRYRHEVFIEQLGWQLDSTHARPQREFDQFDQADTRHILALDTKGQVCGCARLLPTTQPYLLSEVFGFLCDQPSPRSRDTWEVSRFAARALEKGTLPMRVWWNSLHHAWSHGANQVVAVTTPALERYFLKNGVQLSRLGAPQRVNNDHVVALSFPAWQKNGRIALHADSAVA

The amino acid sequence of LuxR family transcriptional regulator (LuxR type):

> P07GM004709 locus = Chr1:5184018:5184668:+ MFEAALNITYELGFEYCGFIMGSNALYRPNRSIHLNNYPDEWNKIYKTENYFEIDPLVVHCKRDVLPLVWEEKTFSAVPDMWAHVQAQGLNFGWAQSVHDFRGFFSMINLGRRKGPVQAHELYEKAGQVLWICHALHAVAAQTYSLGPTFQCPTKLTSRETEILQWSALGKTAADIATILCLSERTVGFHISSAMRKLGVSNKIAAVISAVRNGLF

3.2. Homology modelling

The obtained amino acid sequences by whole genome sequencing of LuxI- and LuxR-type proteins were submitted on SWISS-MODEL to align and construct 3D structures via Blast and HHBlits searches. Alignment results are shown in Fig. S2 (Supplemental material S4). Top-ranked sequences (similarity > 30%) were chosen as templates to build the 3D

structures (Table S3).

The template sequences whose similarity was above 30% for LuxI- and LuxR-type proteins (target protein) of *P. fluorescens* P07 are showed in Table S3. The key residues were conserved in the target protein and template protein sequences. The sequence similarity chart of the templates showed that 3p2h.1.A was closer to the centre point (acyl-homoserine-lactone synthase), while 3sz.t.1.A and 2q0o.1.A were closer to the centre point (LuxR family transcriptional regulators).

The sequence similarity of chain A of 3p2h was 42%. The GMQE score of chain A of 3szt was 0.74. The two scores were higher than those in other models (Table S3) (Supplemental material S5). Thus, chain A of 3p2h and chain A of 3szt were selected as templates to construct 3D models according to the sequence similarity, GMQE (Global Model Quality Estimation) and QMEAN[49] scores. This result was in consonance with the sequence similarity chart.

3.3. Model evaluation

The quality of models was estimated by the QMEAN method and RAMPAGE. The evaluation results are shown in Fig. S3 (Supplemental material S6).

In the local quality plots (Fig. S3, a, g), most of the residues in the two models were above 0.6, indicating that the models were of high quality. In the "Comparison" plot (Fig. S3, b, c, h, i), the Z-score represents the model quality, and the red star represents the model. The red star was in the grey areas with a global QMEAN Z-score between 1 and 2 for LuxI-type proteins (Fig. S3, b, c), whereas it was in light grey areas with a global QMEAN Z-score more than 2 for LuxR-type proteins. The results indicated that the quality of the LuxI-type protein model was better than that of the LuxR-type protein. In the Global QMEAN4 and QMEAN6 quality score plots, the QMEAN4 and QMEAN6 scores were −1.56 and −1.52, −2.44 and −2.07 for the LuxI- and LuxR-type protein models of *P. fluorescens* P07 (Fig. S3, d, e, j, k), respectively. In the Ramachandran plots (Fig. S3, f, l), the residues in the favoured, allowed and outliner regions were 95.6%, 3.2% and 1.3% for the LuxI-type model, while the corresponding values were 97.2%, 2.6% and 0.2% for the LuxR-type protein model.

3.4. Virtual screening

The prepared compounds from the TCM database and furanone C-30 were docked with the built LuxI- and LuxR-type protein models (Supplemental material S7). The Total Score and CScore of furanone C-30 docked with LuxI- and LuxR-type protein of *P. fluorescens* P07 were 3.04, 2, and 2.12, 4, respectively. The compounds whose Total Scores were above 6 and whose C scores were above 4 were selected and are shown in Table 1.

As listed in Table 1, 10 and 12 compounds were selected for the LuxI- and LuxR-type protein models, respectively. Linalyl acetate and citronellyl acetate were selected in both models. Ethyl linalool had the highest docking score of 7.2049. All compounds were prepared to test their MIC, and under the sub-MIC, their anti-quorum sensing activities were measured; the results are shown in Fig. 1.

The MICs of the compounds were tested using the doubling dilution method. The MIC was measured against indicator strains. The results showed that all compounds at the storage concentrations had no antimicrobial activities expect rhodinyl formate (S4) and (−)-beta-citronellol (S12), which showed weak antimicrobial activities. Thus, the MIC was determined to confirm that the two compounds had anti-QS instead of antibacterial activity. The results showed that 50% (v/v) of rhodinyl formate and (−)-beta-citronellol had no inhibitory effect on the two indicator strains. The MIC was 448.5 mg/ml and 428 mg/ml for rhodinyl formate and (−)-beta-citronellol, respectively. Additionally, 70% methanol and 60% DMSO (blank control) showed no inhibitory effect on the indicator strains. The compounds under sub-MIC were applied in QS inhibition assays.

As shown in Fig. 1 (a), the colour of the plate covered with *C. violaceum* CV026 was purple due to CviR expression when C6-HSL was encountered.[50] In Fig. 1 (b), the colour of the plates full of *A. tumefaciens* A136 were blue in the presence of C10-HSL and X-Gal. In the QS inhibitory test, the loss of purple pigmentation and blue colour on the plate treated with the compounds suggested that the compounds could act as QSIs. In contrast, the blank control showed no significant difference. The diameters of the yellowish halos in *C. violaceum* CV026 plates that were treated with benzyl alcohol (S7), (−)-beta-citronellol (S12), ethyl linalool (S1), rhodinyl formate (S4), 1,10-Decanediol (S19), undecanoic acid (S6), 1-Dodecanol (S20), decanal (S17) and houttuynine (S8) were large, indicating that the compounds had strong anti-quorum sensing activities in inhibiting the short chain AHLs. Benzyl alcohol possessed the strongest anti-QS activity. Methyl 3-nonenoate (S22), gamma-dodecalactone (S11), dihydro-beta-ionone (S18), dodecyl aldehyde (S23) and neryl acetate (S21) showed weak anti-QS activities. Similarly, in *A. tumefaciens* A136 plates, the diameters of the yellowish halos in the presence of benzyl alcohol (S7), decanal (S17), 1-Dodecanol (S20), rhodinyl formate (S4) and houttuynine (S8) were larger than that of others, suggesting that these compounds showed strong inhibitory effects on QS. Dodecyl aldehyde (S23), (−)-beta-citronellol (S12), azelaic acid (S15), 1,10-decanediol (S19), undecanoic acid (S6) and dihydro-beta-ionone (S18) showed weak anti-QS activities. These compounds, especially benzyl alcohol, had the ability to inhibit the long chain AHLs.

3.5. Impact of benzyl alcohol on the QS-regulated phenotypes of *P. fluorescens* P07

Benzyl alcohol showed the strongest anti-quorum sensing activities. Besides, benzyl alcohol naturally exists in many plants and it is widely used in the production of industrial chemicals. Most importantly, it was allowed to be used as a food additive in national food safety standard in China. Thus, the influence of benzyl alcohol on the QS-regulated phenotypes of *P. fluorescens* P07 were tested, including swimming and swarming motility, production of extracellular enzymes and siderophores, AHL content, EPS content and biofilm formation. The MIC of benzyl alcohol was measured because of its antibacterial effects on *P. fluorescens* P07. The results showed that the MIC of benzyl alcohol was 0.4% (v/v). Herein, benzyl alcohol at sub-MIC concentrations was used in further tests.

3.5.1. Impact of benzyl alcohol on swimming and swarming motility, production of extracellular enzymes and siderophores

The effect of benzyl alcohol on QS-regulated swimming and swarming motility, extracellular enzymes and siderophore production is shown in Fig. 2.

As shown in Fig. 2 (a and b), *P. fluorescens* P07 migrated from the inoculation point, spread across the plates and formed colonies. A considerable decrease in the migration area was observed by bare eyes in the plates treated with increasing concentrations of benzyl alcohol. In Fig. 2 (c), the plate was blue because of the ternary complex (HDTMA, CAS and Fe^{3+}). Once bacteria produced siderophores, a yellowish halo appeared on the CAS plates owing to the high affinity of the siderophores to Fe^{3+}. There was a yellowish halo around the hole untreated with benzyl alcohol, which suggested that *P. fluorescens* P07 produced siderophores, whereas the size of the yellowish halo decreased when treated with increasing concentrations of benzyl alcohol. Similarly, in the milk plates (Fig. 2 (d)), there was a transparent zone around the hole when the bacteria were untreated with benzyl alcohol because the protein in the plates was broken down by the extracellular protease secreted by *P. fluorescens* P07. The size of the transparent zone treated with increasing concentrations of benzyl alcohol was significantly decreased compared with that of the control.

Table 1
Virtual screening results of QSIs from the TCM database.

Protein	No.	Compound name	Molecular weight	Formula	Compound source	Total Score	Crash	Polar	CScore
LuxI-type protein	S1	Ethyl linalool	182.30	$C_{12}H_{22}O$	*Geranium Wilfordii Maxim.*	7.2049	−1.1012	1.8826	4
	S2	Rosmarinic acid	360.31	$C_{18}H_{16}O_8$	*Mylabris*	6.9031	−0.9413	4.0791	4
	S3	Isopentyl Hexanoate	186.30	$C_{11}H_{22}O_2$	*Hippophae Fructus*	6.7997	−1.4558	1.1452	4
	S4	Rhodinyl formate	184.28	$C_{11}H_{20}O_2$	*Geranium Wilfordii Maxim.*	6.577	−1.3746	1.0799	4
	S5	Citronellyl acetate	198.31	$C_{12}H_{22}O_2$	*Zingiberis Rhizoma*	6.4757	−1.6268	0.9728	5
	S6	Undecanoic acid	186.29	$C_{11}H_{22}O_2$	*Radix Bupleuri*	6.4345	−1.6257	1.6223	4
	S7	Benzyl alcohol	108.14	C_7H_8O	*Chuanxiong Rhizoma*	6.3801	−0.966	0.0191	4
	S8	Houttuynine	198.31	$C_{12}H_{22}O_2$	*Houttuyniae Herba*	6.1463	−0.978	1.3259	4
	S9	2-Undecanone	170.29	$C_{11}H_{22}O$	*Zingiberis Rhizoma*	6.0285	−1.5481	0.3455	4
	S10	Linalyl acetate	196.29	$C_{12}H_{20}O_2$	*Rubi Fructus*	6.0214	−1.2498	0.9945	4
LuxR-type protein	S11	Gamma-Dodecalactone	198.31	$C_{12}H_{22}O_2$	*Sophorae Tonkinensis Radix Et Rhizome*	6.784	−0.3161	0.92	4
	S12	(−)-Beta-citronellol	156.27	$C_{10}H_{20}O$	*Zingiber Officinale Roscoe*	6.7779	−0.5872	0.4995	4
	S13	Linalyl acetate	196.29	$C_{12}H_{20}O_2$	*Myrrha*	6.733	−2.0594	1.0793	5
	S14	Citronellyl acetate	198.30	$C_{12}H_{22}O_2$	*Zingiberis Rhizoma*	6.6508	−1.2166	0.9314	5
	S15	Azelaic acid	188.22	$C_9H_{16}O_4$	*Mahoniae Caulis*	6.6064	−0.6081	2.4843	4
	S16	Tetradecane	198.39	$C_{14}H_{30}$	*Radix Cirsii Japonici*	6.4256	−1.45	0	5
	S17	Decanal	156.27	$C_{10}H_{20}O$	*Herba Taxilli*	6.2775	−0.6755	1.1601	4
	S18	Dihydro-beta-ionone	194.31	$C_{13}H_{22}O$	*Rehmanniae Radix Praeparata*	6.2665	−1.1356	1.1025	4
	S19	1,10-Decanediol	174.28	$C_{10}H_{22}O_2$	*Zingiberis Rhizoma*	6.2619	−0.3803	2.1486	4
	S20	1-Dodecanol	186.33	$C_{12}H_{26}O$	*Panax Ginseng C. A. Mey.*	6.1805	−0.635	1.2065	4
	S21	Neryl acetate	196.29	$C_{12}H_{20}O_2$	*Rose Rugosae Flos*	6.1531	−1.0106	1.8106	4
	S22	Methyl 3-nonenoate	170.25	$C_{10}H_{18}O_2$	*Adenophprae Ae Radix*	6.1336	−1.7459	1.2399	5
	S23	Dodecyl aldehyde	184.32	$C_{12}H_{24}O$	*Codonopsis Radix*	6.0307	−0.8381	1.0851	4

3.5.2. Impact of benzyl alcohol on AHL content

The AHLs produced by *P. fluorescens* P07 were extracted and detected by indicator strains (Fig. 3). GC–MS was applied to quantify the AHL content. The results are shown in Table 2.

As shown in Fig. 3, purple and blue areas appeared in the plates full of the indicator strains, respectively, which indicated that *P. fluorescens* P07 secreted short chain and long chain AHLs. AHLs could be identified both qualitatively and quantitatively by a comparison to the peak time of standard AHLs. From Table 2, *P. fluorescens* P07 produced all kinds of AHLs, most of which was C10-HSL, followed by C14-HSL. However, C12- and C14-HSL were not detected when treated with 0.05% benzyl alcohol. Moreover, the content of C4-, C6- and C10-HSL decreased by 65.86%, 78.79% and 88.20%, respectively, while C8-HSL increased by 69.84% compared with control. C8-, C10-, C12- and C14-HSL were not detected when *P. fluorescens* P07 was treated with 0.1% benzyl alcohol. The content of C4- and C6-HSL decreased by 91.20% and 72.20%, respectively. C6-, C11- and C14-HSL were not found, and the content of the other AHLs was relatively lower than that of the control when *P. fluorescens* P07 was treated with 0.15% benzyl alcohol.

3.5.3. Impact of benzyl alcohol on biofilm formation

Changes in the biofilm formation of *P. fluorescens* P07 treated with different concentrations of benzyl alcohol were observed by SEM (scanning electron microscope) and CLSM (confocal laser scanning microscope) (Fig. 4).

As shown in Fig. 4, the strain of *P. fluorescens* P07 aggregated together to form large clusters, and the biofilm was rather thick and compact when the bacteria were untreated with benzyl alcohol. The biofilm was thinner than that of the control when the bacteria were treated with 0.05% benzyl alcohol, but there were still netlike biofilms.

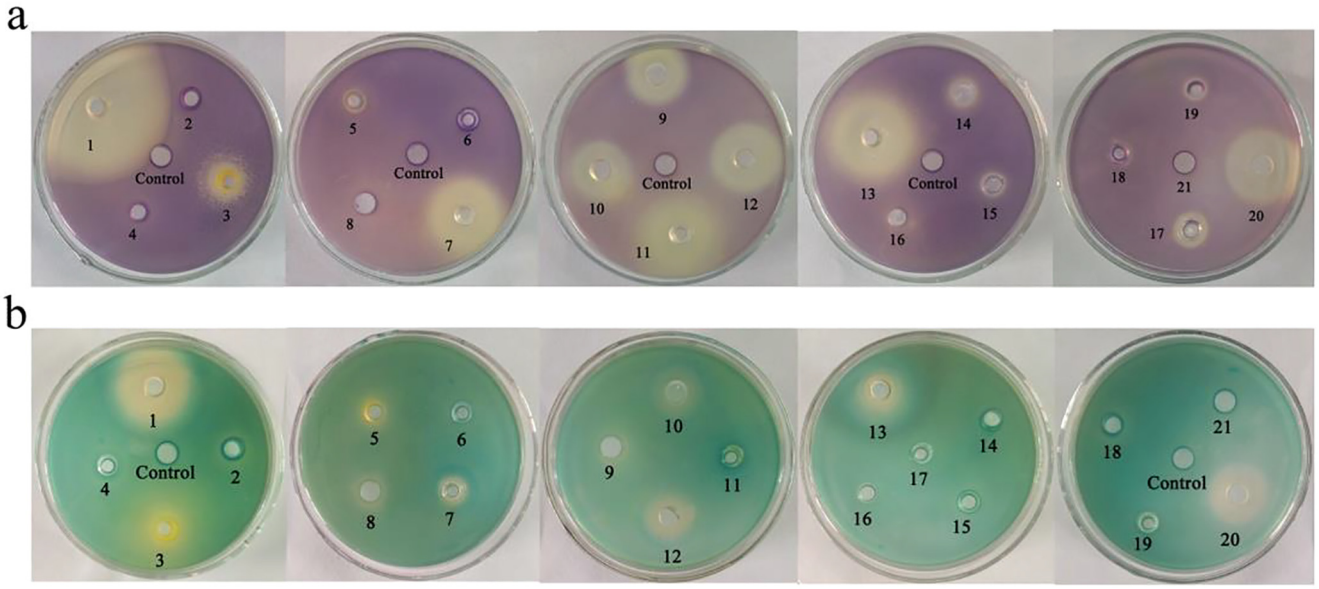

Fig. 1. Anti-quorum sensing activities of selected compounds tested by indicator strains (a: *C. violaceum* CV026; b: *A. tumefaciens* A136). The numbers in the figure represent the following: 1: S7; 2: S3; 3: S17; 4: S10; 5: S23; 6: S16; 7: S12; 8: S15; 9: S19; 10: S6; 11: S1; 12: S20; 13: S4; 14: S11; 15: S22; 16: S14; 17: S21; 18: S9; 19: S18; 20: S8; 21: S2.

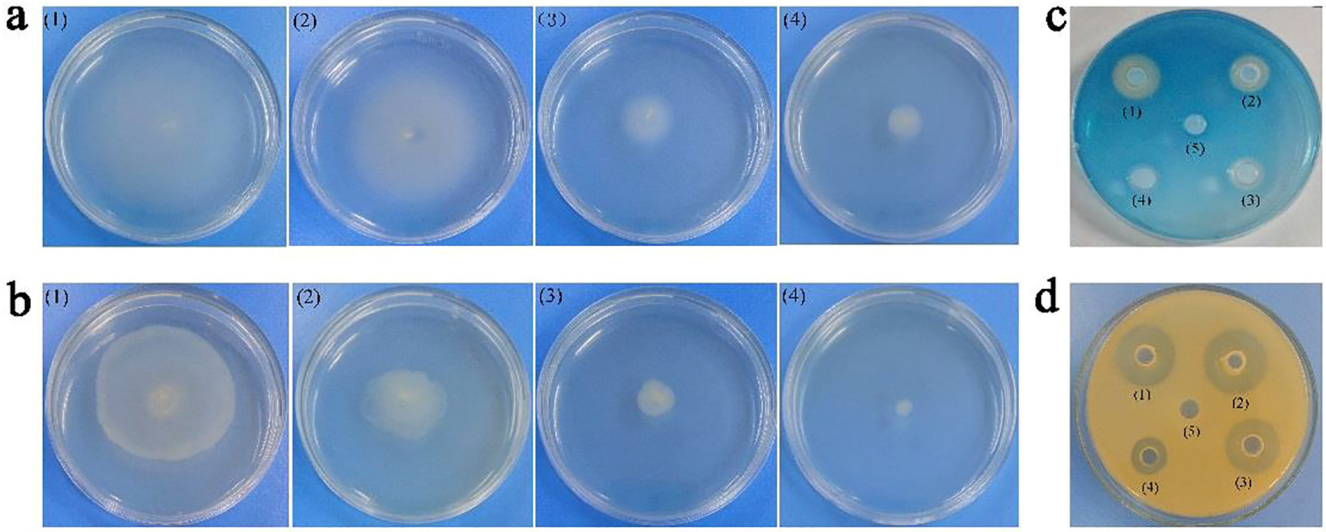

Fig. 2. Effect of benzyl alcohol on swimming (a) and swarming (b) motility, production of siderophores (c) and extracellular enzymes (d) of *P. fluorescens* P07. The numbers in the figure represent the following: 1: control; 2: 0.05% benzyl alcohol; 3: 0.10% benzyl alcohol; 4: 0.15% benzyl alcohol; 5: 70% methanol was served as blank control.

The biofilms were few when *P. fluorescens* P07 was treated with 0.1% benzyl alcohol. The most obvious changes in biofilm were observed when the bacteria were treated with 0.15% benzyl alcohol; the cell aggregations were scattered, and almost no biofilms were formed. The images obtained from CLSM were consisted with the results of SEM. The deeper the green colour, the greater the biofilm content. The deepest colour was observed when the bacteria were untreated with benzyl alcohol, indicating that the biofilm was very thick and dense. The colour became lighter when the bacteria were treated with increasing concentrations of benzyl alcohol.

To quantify the biofilms produced by *P. fluorescens* P07 treated with different concentrations of benzyl alcohol, the absorbance (590 nm) was measured, and the results are shown in Fig. 5.

In the qualitative analysis, benzyl alcohol showed a concentration-dependent inhibition in the biofilm formation of *P. fluorescens* P07. The biofilm was inhibited up to 90.42% by benzyl alcohol at the concentration of 0.15% ($p < 0.01$). The results were in accordance with the morphological observation.

3.5.4. Impact of benzyl alcohol on EPS content

Changes in the EPS content of *P. fluorescens* P07 treated with different concentrations of benzyl alcohol were determined by Raman spectrum technology (Fig. 6). The Raman band assignments of the reference compounds are listed in Table 3.

Raman spectra showed that the main chemical compositions of the EPSs were protein, carbohydrate, nucleic acids and lipids. Bands in the range of 720–730 cm^{-1} and 810–820 cm^{-1}, which were typical of vibrations of adenine, tryptophan and nucleic acid structures, respectively, were identified in the EPSs of *P. fluorescens* P07 in the absence of benzyl alcohol. These vibrations are caused by CH_2 and C-O-P-O-C linkages. Between 1030 and 1130 cm^{-1}, deformation vibrations of carbohydrates, which were caused by -C—C-, C-O and C-O-H groups, were allocated. Between 1200 and 1343 cm^{-1}, the deformation vibrations of N—H and C—H groups were identified, and these regions were typical for structural elements linked to proteins. Additionally, characteristic bands between 1650 and 1680 cm^{-1} showed that amide I and unsaturated lipids were allocated. At a higher Raman shift from 1855 up to 2920 cm^{-1}, the stretching vibrations of CH_2 groups, CH_3 groups, sporopollenin and lipids were determined. However, when *P. fluorescens* P07 was treated with different concentrations of benzyl alcohol, the corresponding chemical compounds in the EPS decreased. In addition, the higher the concentrations of benzyl alcohol, the weaker was the intensity of the EPS Raman spectra (Fig. 6).

3.6. Docking analysis

Ligand-receptor interactions of benzyl alcohol and the LuxI-type protein of *P. fluorescens* P07 were analysed by molecular docking. As shown in Fig. 7 (a and b), the 3D structure of benzyl alcohol was fit into the active site and formed important protein–ligand interactions with the key residues of the LuxI-type protein of *P. fluorescens* P07. The two-dimensional interaction plot clearly showed that benzyl alcohol formed conventional hydrogen bonds, pi-donor hydrogen bonds and pi-alkyl bonds with ARG 105, VAL 139, LEU81 and ALA 138, respectively. The others are mainly van der Waals interactions. Other compounds with potent anti-QS activities such as ethyl linalool, rhodinyl formate, houttuynine and (−)-beta-citronellol were also docked with LuxI-type protein and formed important interactions (Fig. 7, d-g). Benzyl alcohol also formed conventional hydrogen bond and pi-donor hydrogen bond with known LuxI-type protein, namely, LasI of *Pseudomonas aeruginosa*. Benzyl alcohol was docked with LuxR-type protein and the Total Score was 3.0793 and CScore was 1.

4. Discussion

P. fluorescens exists widely in nature and is found in plants, soil, water and surfaces. It can produce soluble fluorescent pigment pyoverdine. *P. fluorescens* not only is a food spoilage bacteria but also causes diseases in humans, such as infections in immuno-compromised patients,[59] and is a cause of fin rot in fish. More seriously, several *P. fluorescens* strains have emerged with drug resistance to ampicillin and streptomycin.[60] In this study, *P. fluorescens* P07 was isolated from deteriorated turbot (*Scophthalmus maximus*) which is an important marine aquaculture fish in China during cold storage. Thus, interfering with the QS system of *P. fluorescens* P07 may be a novel way to preserve refrigerated aquatic products and control infections. TCM has a long history, and the toxicities and side effects are relatively milder and the costs are lower. Moreover, in European markets, TCMs are often classified as “healthcare products” or “food”, rather than “drugs”. Therefore, screening for QSIs from the TCM database has unique advantages. The compounds in our study were derived from the Traditional Chinese Medicine Systems Pharmacology Database and Analysis Platform (TCMSP), which is one of the most comprehensive and largest non-

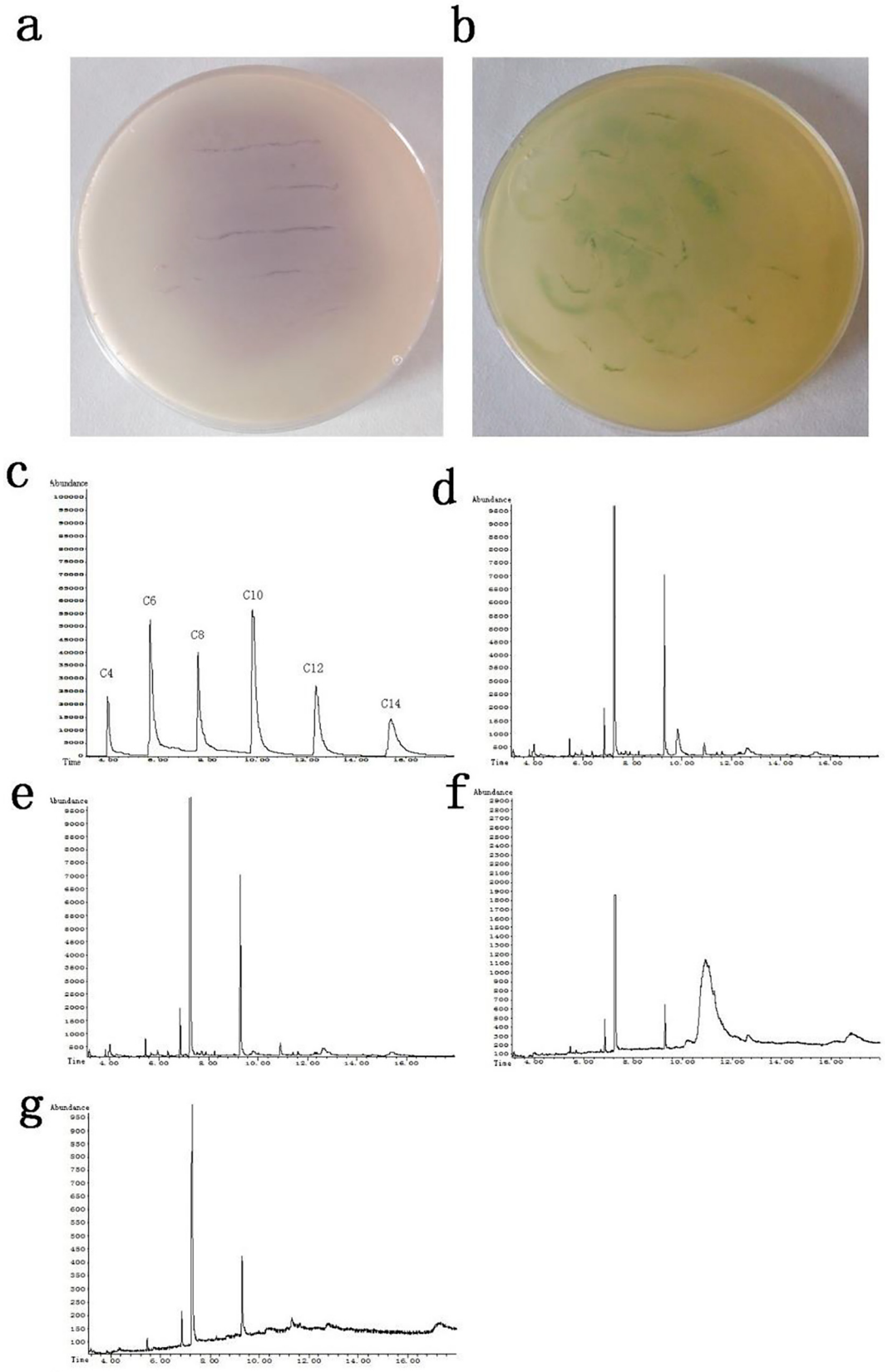

Fig. 3. Detection of AHLs produced by *P. fluorescens* P07 through indicator strains (a: *C. violaceum* CV026; b: *A. tumefaciens* A136) and GC–MS chromatograms (c-g). c: Standard AHLs (2 μg/ml); d: Control; e: 0.05% benzyl alcohol; f: 0.10% benzyl alcohol; g: 0.15% benzyl alcohol.

Table 2
Influence of benzyl alcohol on AHL content.

AHLs	Peak time	Standard AHLs	Control	0.05% benzyl alcohol	0.10% benzyl alcohol	0.15% benzyl alcohol
		Peak area				
C4-HSL	3.961	1,207,212 ± 117,795	18,151 ± 1549	6197 ± 1143	1599 ± 475	62 ± 43
C6-HSL	5.663	6,974,961 ± 612,084	14,521 ± 1033	3080 ± 870	4037 ± 647	–
C8-HSL	7.606	3,287,476 ± 705,961	3200 ± 444	10,609 ± 3203	–	969 ± 106
C10-HSL	9.823	6,712,817 ± 505,514	127,031 ± 9415	14,991 ± 657	–	598 ± 52
C12-HSL	12.390	3,801,340 ± 656,806	19,688 ± 1658	–	–	–
C14-HSL	15.415	3,047,095 ± 668,409	35,202 ± 5681	–	–	–

–: Dot detected.

commercial TCM databases available for download in the world. Approximately 499 kinds of herbal medicines and their chemical compositions are included in the database (13144 molecules and 29,384 compounds).

Since the 3D (three-dimensional) structure of LuxI- and LuxR-type proteins of *P. fluorescens* P07 was not found in PDB (Protein Data Bank) database, thus, homology modelling was used to build the structure of the two proteins. The amino acids for homology modelling were obtained by whole-genome sequencing. The whole-genome sequencing offered large amounts of information on *P. fluorescens* P07. The whole genome of *P. fluorescens* P07 drawn by Circos software was circular, in which information such as the gene functional annotation and the ncRNA and G + C content were displayed. The amino acids of the two proteins were submitted to SWISS-MODEL for homology modelling. The sequence identity and similarity as well as the target sequence coverage were obtained through sequence alignment; the results revealed that the residues in the active site of the target protein and template proteins were strictly conserved. Global Model Quality Estimation (GMQE) is used for quality evaluation. The higher the score, the higher is the model reliability. QMEAN can provide global and local absolute-quality evaluations. Thus, on the basis of the QMEAN and GMQE scores, 3p2h and 3szt were chosen as templates for LuxI- and LuxR-type protein models.

It is very important to assess the quality of built protein models. The QMEAN method and RAMPAGE were used to evaluate the two built models. There are two global score values, *i.e.,* QMEAN4 and QMEAN6,[61] in the QMEAN method. QMEAN4 is a reliable score that contains four statistical potential terms. Two agreement terms were added to the QMEAN6 score to estimate the consistency of sequence-based predictions with structural features. The QMEAN4 and QMEAN6 scores indicated that the two built models of *P. fluorescens* P07 were of good quality. The QMEAN Z-score represents the consistency of the experimental structure and model structure. The Z-score of the two built models of *P. fluorescens* P07 were both higher than -4.0, indicating that the two models were valid. Additionally, the Ramachandran plots also suggested that the two built models were reliable and of good quality and that they could predict the target proteins well. Similarly, Hollingsworth et al. created models of gp 120 protein from HIV-1 strains by homology modelling. The structural properties of the built

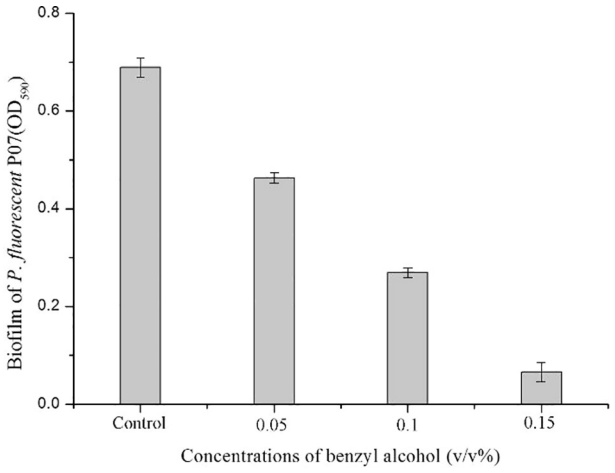

Fig. 5. Effect of benzyl alcohol on biofilm formation of *P. fluorescens* P07.

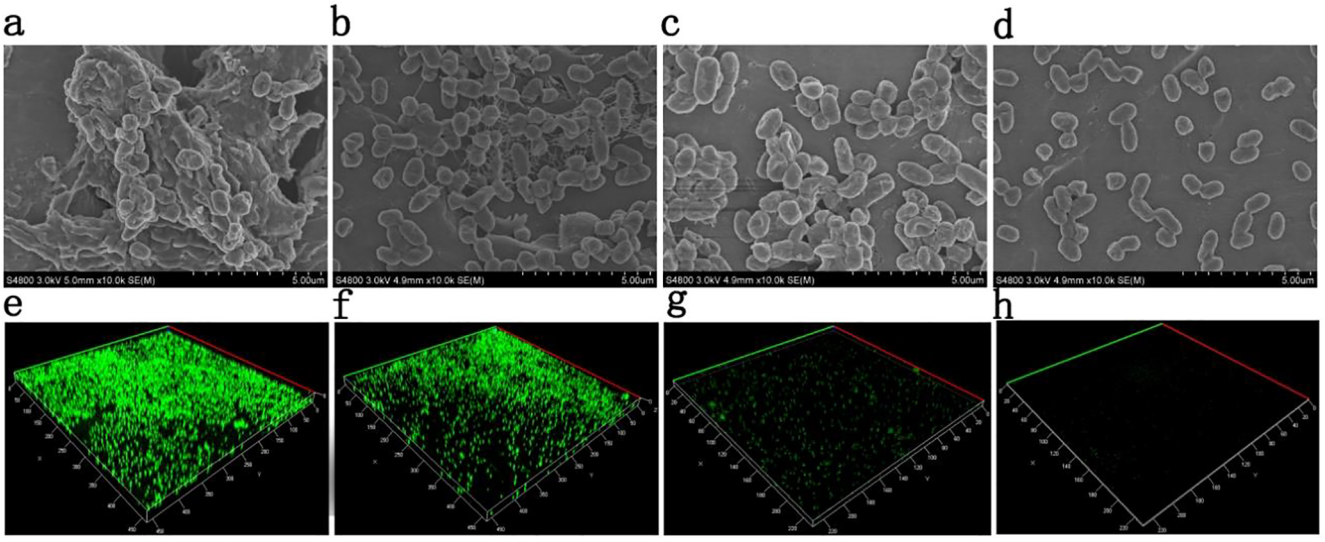

Fig. 4. Effect of benzyl alcohol on biofilm formation of *P. fluorescens* P07 observed by SEM (a–d) and CLSM (e–h). a, e: Control; b, f: 0.05% benzyl alcohol; c, g: 0.10% benzyl alcohol; d, h: 0.15% benzyl alcohol.

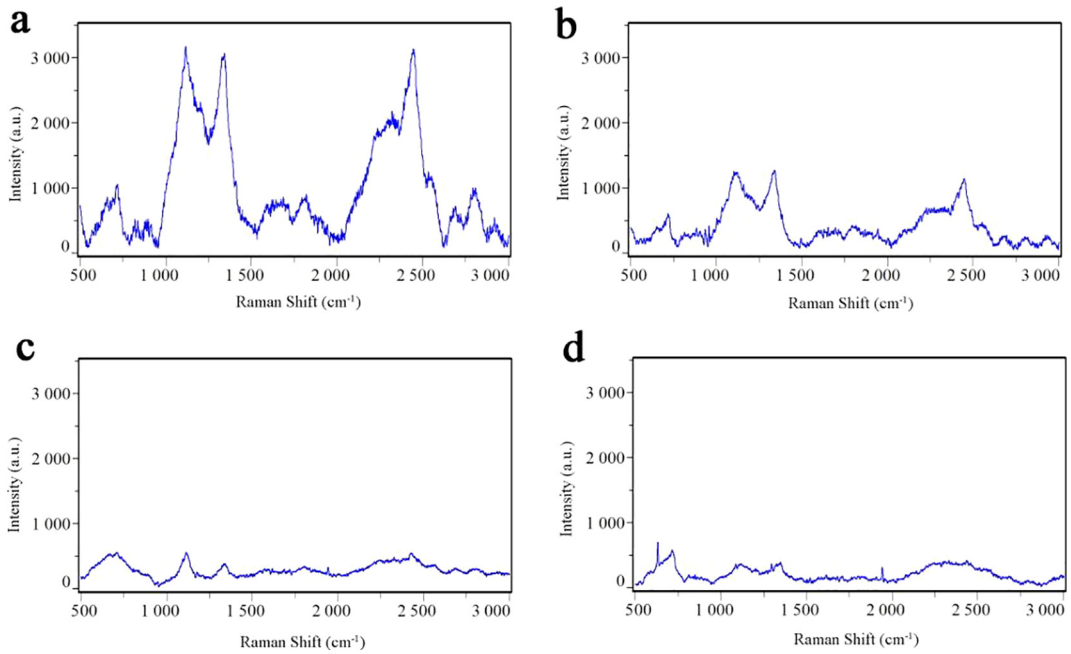

Fig. 6. Raman spectrum of the EPSs of *P. fluorescens* P07 treated with benzyl alcohol. a: control; b: 0.05% benzyl alcohol; c: 0.10% benzyl alcohol; d: 0.15% benzyl alcohol.

Table 3
Assignment of Raman bands in biofilms.

Band or band range (cm^{-1})	Assigned to	Reference
544–553	Carbohydrate	51,52
~600	Arom ring def sporopollenin, phenylalanine	
720–730	CH_2, adenine; ring breath tryptophan	
810–820	C-O-P-O-C in RNA, nucleic acids	
820–860	C-C str, C-O-C glycosidic link, C-O-P-O-C in RNA	
855–899	C-O-C 1,4 glycosidic link, C-C str	51
1001–1005	Phenylalanine	53
1030–1130	Carbohydrates, mainly –C-C-, C-O, C-O-H def	
1145–1160	C-C, C-O ring breath, asymm	54
1200–1290	Amide III	
~1300	N-H, C-H def, amide III	
~1320	Protein (amide III); C-H def	55
~1327	Protein (amide III); C-H def	
1343	Protein (amide III)	56
1400–1420	COO^- symm	
1440–1460	CH_2 def	57
1574	Guanine, adenine (ring stretching)	
1583	Guanine, adenine ring str	
~1600	Arom ring str, sporopollenin, phenylalanine	53
1605–1620	C=C Tyrosine, tryptophan, phenylalanine	
1540–1650	COO^- asymm	55
1650–1680	Amide I and unsaturated lipids	
1725–1750	C=O str	
2920–1855	CH_2, CH_3 str, sporopollenin, lipids	58
2935	CH_2 str asymmetric	

str: stretching; def: deformation; arom: aromatic.

models were also evaluated by Ramachandran plots and ANOLEA scores.[62]

The 3D structures of the compounds from the TCM database were docked with the prepared models of *P. fluorescens* P07. Total Score was the total Surflex-Dock score expressed as $-\log(K_d)$. CScore (Consensus Score) was computed from the Surflex-Dock Total Score and the additional scoring functions.[63] CScore integrates a number of popular scoring functions for ranking the affinity of ligands bound to the active site of a receptor. CScore always reports the output of the docking engine as Total Score.[64] CScore can range from 0 to 5, where 5 indicates that a ligand was judged good by all functions. Structures with scores of 3, 4 or 5 merit further consideration. Structures with a consensus score of 0 are consistently considered bad by all scoring functions and should be dropped.[65] Generally, compounds with Total Score over 6 and C Score over 4 would be considered to be tested for their activities. As control, the docking score of furanone C-30 was lower that of many other compounds in the TCM database. Thus, the top-ranked compounds, for which the docking scores were higher than 6 and the C scores were higher than 4, were selected to test their anti-QS activities. Before the anti-QS test, MICs of the compounds were determined to ensure that the compounds acted on the QS instead of bacteriostatic effect. Usage of biosensors made rapid screening of QSIs possible. The loss of purple pigment and blue colour in the holes supplemented with the compounds in the plates full of the two biosensors, respectively, indicated that these compounds were able to inhibit the production of short chain and long chain AHLs. Furthermore, the halo zone around the hole was opaque, which also indicated that the bacterial growth was not affected by the compounds. Several compounds such as benzyl alcohol, (−)-beta-citronellol and ethyl linalool had strong anti-quorum sensing activities. The hit rate indicated that screening the QSIs from the TCM database by the virtual screening method was quite feasible. (−)-beta-citronellol was extracted from *Zingiber officinale Roscoe*, which is used to flavour meals and is also a very popular traditional Chinese medicine used to treat typhoid fever. Ethyl linalool and rhodinyl formate were obtained from *Geranium wilfordii Maxim*, a popular traditional Chinese medicine that is effective in the treatment of rheumatism. 1-Dodecanol is from *Panax Ginseng C. A. Mey.*, an extremely valued traditional Chinese medicine, which has shown various bioactivities, such as anti-aging, anti-diabetic, immunoregulatory, anticancer, *etc.*[66] Undecanoic acid, 1,10-decanediol, decanal and houttuynine were from *Radix Bupleuri, Zingiberis Rhizoma, Herba Taxilli* and *Houttuyniae Herba*, respectively. These are all common traditional Chinese medicines. Among them, benzyl alcohol particularly displayed a strong ability in inhibiting both the short chain and long chain AHLs. Benzyl alcohol is from *Chuanxiong Rhizoma*, which is also a valued traditional Chinese medicine. It is an aromatic alcohol with a mild

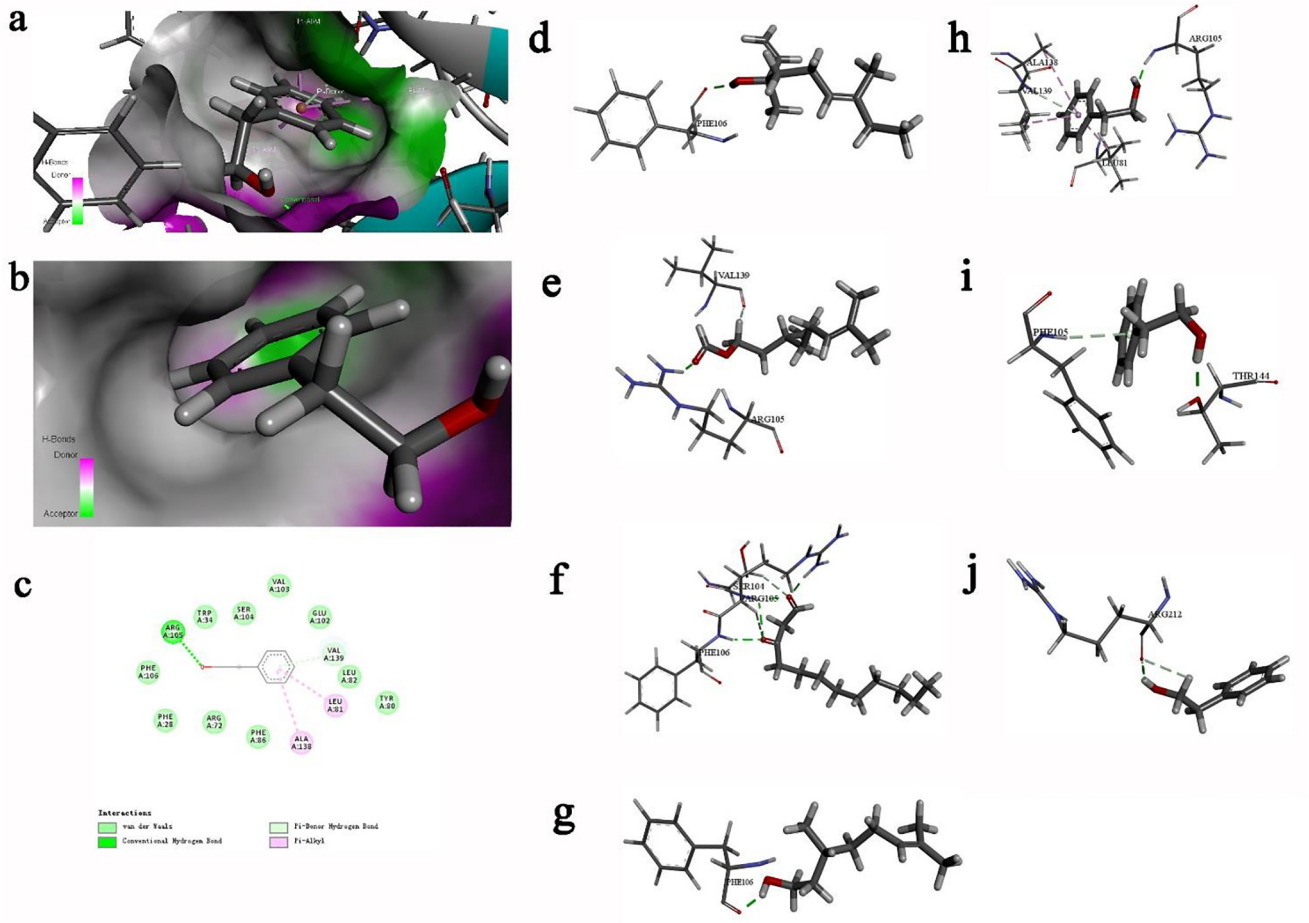

Fig. 7. Graphical representations of the ligand-protein interactions. (a) The schematic overview of the interactions between benzyl alcohol and nearby binding site residues; (b) The three-dimensional H-bond surface plot in the docking box; (c) The two-dimensional interaction plot; (d); Interactions between ethyl linalool and LuxI-type protein (e) Interactions between rhodinyl formate and LuxI-type protein; (f) Interactions between houttuynine and LuxI-type protein; (g) Interactions between (−)-beta-citronellol and LuxI-type protein; (h) Interactions between benzyl alcohol and LuxI-type protein; (i) Interactions between benzyl alcohol and LasI protein; (j) Interactions between benzyl alcohol and LuxR-type protein.

aromatic fragrance, which is found in many plants, fruits and teas as well as a variety of essential oils. Studies have shown that the acute toxicity of benzyl alcohol is low and the LD_{50} value is 1.2 g/kg in rats. Furthermore, there was no evidence that benzyl alcohol is carcinogenic, teratogenic or reproductive.[67] Thus, further tests were carried out to study the impact of benzyl alcohol on the QS-regulated phenotypes of *P. fluorescens* P07, such as swimming and swarming motility, production of siderophores and extracellular enzymes, biofilm formation, EPS content and AHLs production.

P. fluorescens has multiple flagella for motion. Swimming and swarming motility are flagella-dependent motilities regulated by the QS system. The two motilities were of great importance in the first stage of biofilm formation to allow bacterial spread on surfaces.[17] Photographic images of swimming and swarming motilities of *P. fluorescens* P07 treated with different concentrations of benzyl alcohol indicated that the two QS-regulated motilities were significantly inhibited by benzyl alcohol. The results of our study were comparable with that of Gopu et al. They found that the swimming and swarming motilities of *Yersinia enterocolitica* and *Pseudomonas aeruginosa* were significantly restrained by quercetin.[15] Siderophores are secondary metabolites excreted by bacteria under iron-deficient conditions. Siderophores have a high affinity to Fe^{3+} and are used by bacteria used to collect iron from the environment.[68] Similarly, the production of siderophores was also controlled by QS system.[69] Photographic images of CAS plates suggested that benzyl alcohol had the ability to inhibit siderophore production of *P. fluorescens* P07. Heat-tolerant protease and lipase produced by psychrotrophic bacteria are the main reasons resulting in food spoilage.[70] The secreted proteases by *P. fluorescens* degraded proteins into volatile nitrogen- and sulfur-containing compounds and resulted in food spoilage. The figure shows that benzyl alcohol had an inhibitory effect on the extracellular enzyme production of *P. fluorescens*. Zhu and co-workers found that extracellular protease production in *Shewanella baltica* XH2 was significantly inhibited by green tea polyphenols.[71]

Gram-negative bacteria such as *P. fluorescens* use small diffusible signalling molecules, *i.e.,* AHLs, as indicators of population density to coordinate gene expression. Hence, controlling or eliminating the AHLs might be an alternative strategy to control the QS system. AHL consists of a fatty acyl chain and a lactonized homoserine, and different bacteria may secrete AHLs varying in their carbon and *N*-acyl chains. It has been reported that some other *Pseudomonas* spp. produce different AHLs. Liu et al. found that *P. fluorescens* strain 395 produces C4-HSL and 3OC8-HSL[72], while two strains of *P. fluorescens* isolated by Maurilio et al. from refrigerated raw milk did not produce AHLs.[1] In our study, through biosensor strain tests, it was shown that *P. fluorescens* 07 produced both short chain and long chain AHLs. Quantitative and qualitative analysis of AHLs when bacteria were treated with different concentrations of benzyl alcohol were performed by GC–MS. Through GC–MS, benzyl alcohol was found to significantly decrease the AHL production of *P. fluorescens* 07.

Biofilms are very prevalent in nature and in industrial and hospital settings. Biofilms can adhere to living or non-living surfaces. In

addition, once formed, they are very hard to eradicate.[73] Biofilms are problematic in food industries because they can form on food equipment, causing food contamination and spoilage. Worse, biofilms also pose health risks to consumers, such as outbreaks of food borne pathogens.[74] Since QS has been reported to be related to biofilm formation, interfering with the bacterial QS system would control biofilm formation.[75,76] Morphological observation through SEM clearly showed that *P. fluorescens* 07 organisms were good biofilm producers that produced dense and compact biofilms. When *P. fluorescens* 07 was treated with increasing concentrations of benzyl alcohol, the biofilms decreased, indicating that benzyl alcohol had the ability to inhibit the formation of biofilms. Additionally, the bacterial morphologies were normal, which also suggested that benzyl alcohol acted as a QSI rather than exhibiting antibacterial activity. CLSM is a great tool to characterize biofilm structures and is a supplement to SEM. The result of CLSM is in alignment to that of SEM as well as to the quantitative analysis of the biofilms. Similarly, Zhang et al. extracted polyphenolic compounds from *Rosa rugosa* tea and found that these compounds inhibit biofilm formation up to 72.90% and 67.02% in *Pseudomonas aeruginosa* PAO1 and *Escherichia coli* K-12, respectively.[23]

Adherent bacteria are encased in extracellular polymeric substances to resist detergents and antibiotics. In some cases, antibiotic resistance can be increased a thousandfold.[9,77] EPSs mainly consist of extracellular polysaccharides, proteins and nucleic acids.[78] Raman microscopy (RM) has become a very useful tool to detect the chemical constituents of EPSs. It is time-saving and does not require complicated pretreatment, which reduces the risk of changing the structure and substances of biofilms. The chemical changes in EPSs when treated with benzyl alcohol indicated that benzyl alcohol affected the content of bacterial extracellular components that directly influence the biofilm development of *P. fluorescens* 07.

The inhibitory mechanism of benzyl alcohol could be known by analyzing the ligand–protein interactions. Basically, benzyl alcohol formed conventional hydrogen bonds, pi-donor hydrogen bonds and pi-alkyl bonds with ARG 105, LEU 81, ALA 138 and VAL 139 of LuxI-type protein. Benzyl alcohol was docked with LasI protein of *Pseudomonas aeruginosa* which 3D structure has been identified and it also formed conventional hydrogen bond and pi-donor hydrogen bond with PHE 105 and THR 144, respectively. The results suggested that benzyl alcohol had a similar combination pattern with LuxI-type protein. Moreover, ethyl linalool, houttuynine and (−)-beta-citronellol all formed conventional hydrogen bond with PHE 106 of LuxI-type protein, suggesting that the PHE 106 was quite important in the active site. Besides, rhodinyl formate formed conventional hydrogen bond and carbon hydrogen with ARG 105 and VAL 139, respectively. Similarly, houttuynine formed conventional hydrogen with ARG 105. All above results indicated that VAL 139 and ARG 105 were vital residues in the active site of LuxI-type protein. The interactions between benzyl alcohol and LuxI-type protein were more than that of other compounds, leading to the strong affinity of LuxI-type for benzyl alcohol, which may be the main reason for the most potent anti-QS activity of benzyl alcohol. The low Total Score and CScore of benzyl alcohol docked with LuxR-type protein could also prove the selectivity and strong affinity of benzyl alcohol for LuxI-type protein. AHLs bind to the LuxR-type proteins and induce target gene expression in gram-negative bacteria. Thus, the anti-QS activity of benzyl alcohol on *P. fluorescens* P07 might be because that the benzyl alcohol was closely combined to LuxI-type protein, blocking the production of AHLs and, thus, eventually interfering with the QS circuit of *P. fluorescens* P07.

5. Conclusion

P. fluorescens grows or reproduces in food at refrigeration temperatures, thereby causing food spoilage; moreover, the bacterium also causes diseases in humans. Therefore, a promising strategy may target the QS system of the bacterium to control its spoilage potential and pathogenicity. Summarizing our study, we can conclude that the discovery of QSIs from a TCM database through receptor-based virtual screening for *P. fluorescens* P07 was feasible and that the hit rate was high. Various bioactive compounds have been identified to have QS inhibitory activities. In addition, further experiments validated that benzyl alcohol possessed strong anti-quorum sensing activities in *P. fluorescens* P07. Furthermore, the built LuxI and LuxR protein models of *P. fluorescens* P07 through homology modelling were effective targets for the discovery of bioactive QSIs.

Acknowledgements

This research was financially supported by the National Natural Science Foundation of China (No. 31471639; 31301572) and National Key Research and Development Program of China (2017YFD0400106).

Competing interests statement

All authors declare no conflict of interest.

A. Supplementary data

Supplementary data associated with this article can be found, in the online version, at http://dx.doi.org/10.1016/j.bmc.2018.06.039. These data include MOL files and InChiKeys of the most important compounds described in this article.

References

1. Maurilio L, Martins U, Pinto M, et al. Lack of AHL-based quorum sensing in *Pseudomonas fluorescens* isolated from milk. *Braz J Microbiol.* 2014;45:1039–1046.
2. Wei HL, Zhang LQ. Quorum-sensing system influences root colonization and biological control ability in *Pseudomonas fluorescens* 2P24. *Antonie Van Leeuwenhoek.* 2006;89:267–280.
3. Stellato G, Utter DR, Voorhis A, De Angelis M, Eren AM, Ercolini D. A few *pseudomonas oligotypes* dominate in the meat and dairy processing environment. *Front Microbiol.* 2017;8:264.
4. Liu X, Shen B, Du P, et al. Transcriptomic analysis of the response of *Pseudomonas fluorescens* to epigallocatechin gallate by RNA-seq. *PLoS One.* 2017;12:e0177938.
5. Lu G, Luhr J, Stoecklein A, Warner P, Tapprich W. Complete genome sequences of *Pseudomonas fluorescens* bacteriophages isolated from freshwater samples in Omaha, Nebraska. *Genome Announc.* 2017;5.
6. Myszka K, Schmidt MT, Majcher M, Juzwa W, Olkowicz M, Czaczyk K. Inhibition of quorum sensing-related biofilm of *Pseudomonas fluorescens* KM121 by *Thymus vulgare* essential oil and its major bioactive compounds. *Int Biodeterior Biodegrad.* 2016;114:252–259.
7. Yang X, Zhang Q, Chen ZY, Liu H, Li P. Investigation of *Pseudomonas fluorescens* strain 3JW1 on preventing and reducing aflatoxin contaminations in peanuts. *PLoS One.* 2017;12:e0178810.
8. Goncalves L, Piccoli RH, Peres AP, Saude AV. Predictive modeling of *Pseudomonas fluorescens* growth under different temperature and pH values. *Braz J Microbiol.* 2017;48:352–358.
9. Yan Q, Gao W, Wu XG, Zhang LQ. Regulation of the PcoI/PcoR quorum-sensing system in *Pseudomonas fluorescens* 2P24 by the PhoP/PhoQ two-component system. *Microbiology.* 2009;155:124–133.
10. Brown D. A mathematical model of the Gac/Rsm quorum sensing network in *Pseudomonas fluorescens*. *Biosystems.* 2010;101:200–212.
11. Zhu S, Wu H, Zeng M, Liu Z, Wang Y. The involvement of bacterial quorum sensing in the spoilage of refrigerated *Litopenaeus vannamei*. *Int J Food Microbiol.* 2015;192:26–33.
12. Truchado P, Larrosa M, Castro-Ibáñez I, Allende A. Plant food extracts and phytochemicals: their role as quorum sensing inhibitors. *Trends Food Sci Technol.* 2015;43:189–204.
13. Park S, Kim HS, Ok K, Kim Y, Park HD, Byun Y. Design, synthesis and biological evaluation of 4-(alkyloxy)-6-methyl-2H-pyran-2-one derivatives as quorum sensing inhibitors. *Bioorg Med Chem Lett.* 2015;25:2913–2917.
14. Nam A, Kweon J, Ryu J, Lade H, Lee C. Reduction of biofouling using vanillin as a quorum sensing inhibitory agent in membrane bioreactors for wastewater treatment. *Membr Water Treat.* 2015;6:189–203.
15. Gopu V, Meena CK, Shetty PH. Quercetin influences quorum sensing in food borne bacteria: *in-vitro* and *in-silico* evidence. *PLoS One.* 2015;10:e0134684.
16. Kumar NV, Murthy PS, Manjunatha JR, Bettadaiah BK. Synthesis and quorum sensing inhibitory activity of key phenolic compounds of ginger and their derivatives. *Food Chem.* 2014;159:451–457.
17. El-Mowafy SA, Abd El Galil KH, El-Messery SM, Shaaban MI. Aspirin is an efficient inhibitor of quorum sensing, virulence and toxins in *Pseudomonas aeruginosa*. *Microb Pathog.* 2014;74:25–32.

18. Batista D, Carvalho AP, Costa R, Coutinho R, Dobretsov S. Extracts of macroalgae from the Brazilian coast inhibit bacterial quorum sensing. *Botanica Marina.* 2014;57.
19. des Essarts YR, Sabbah M, Comte A, et al. N,N′-alkylated Imidazolium-derivatives act as quorum-sensing inhibitors targeting the Pectobacterium atrosepticum-induced symptoms on potato tubers. *Int J Mol Sci.* 2013;14:19976–19986.
20. Chu W, Zhou S, Jiang Y, Zhu W, Zhuang X, Fu J. Effect of traditional Chinese herbal medicine with antiquorum sensing activity on *Pseudomonas aeruginosa*. *Evid Based Complement Alternat Med.* 2013;2013:648257.
21. Issac Abraham Sybiya Vasantha Packiavathy PA. Khadar Syed Musthafa, Shunmugiah Karutha Pandian, Arumugam Veera Ravi. Antibiofilm and quorum sensing inhibitory potential of *Cuminum cyminum* and its secondary metabolite methyl eugenol against Gram negative bacterial pathogens. *Food Res Int.* 2012;45:85–92.
22. Choo JH, Rukayadi Y, Hwang JK. Inhibition of bacterial quorum sensing by vanilla extract. *Lett Appl Microbiol.* 2006;42:637–641.
23. Zhang J, Rui X, Wang L, Guan Y, Sun X, Dong M. Polyphenolic extract from *Rosa rugosa* tea inhibits bacterial quorum sensing and biofilm formation. *Food Control.* 2014;42:125–131.
24. Packiavathy IA, Priya S, Pandian SK, Ravi AV. Inhibition of biofilm development of uropathogens by curcumin – an anti-quorum sensing agent from *Curcuma longa*. *Food Chem.* 2014;148:453–460.
25. Lin SH, Huang KJ, Weng CF, Shiuan D. Exploration of natural product ingredients as inhibitors of human HMG-CoA reductase through structure-based virtual screening. *Drug Des Devel Ther.* 2015;9:3313–3324.
26. Sommer T, Hubner H, El Kerdawy A, Gmeiner P, Pischetsrieder M, Clark T. Identification of the beer component hordenine as food-derived dopamine D2 receptor agonist by virtual screening a 3D compound database. *Sci Rep.* 2017;7:44201.
27. Koh KH, Tham FY. Screening of traditional Chinese medicinal plants for quorum-sensing inhibitors activity. *J Microbiol Immunol Infect.* 2011;44:144–148.
28. Nie J, Zhao C, Deng LI, et al. Efficacy of traditional Chinese medicine in treating cancer. *Biomed Rep.* 2016;4:3–14.
29. Tang JLTW. The need to evaluate the clinical effectiveness of traditional Chinese medicine. *Hong Kong Med J.* 1998;4:208–210.
30. Wee YCKH. *An illustrated dictionary of traditional Chinese medicines.* Singapore: Times Publishing; 1990.
31. Shaw Paul D, Ping G, Daly Sean L, et al. Detecting and characterizing *N*-acyl-homoserine lactone signal molecules by thin-layer chromatography. *Proc Natl Acad Sci USA.* 1997;94:6036–6041.
32. Konstantin Berlin SK, Chin Chen-Shan, Drake James, Landolin Jane M, Phillippy Adam M. Assembling large genomes with single-molecule sequencing and locality sensitive hashing. *Nat Biotechnol.* 2015;33:623–630.
33. Koren S, Phillippy AM. One chromosome, one contig: complete microbial genomes from long-read sequencing and assembly. *Curr Opin Microbiol.* 2015;23:110–120.
34. Ashburner M, Ball CA, Blake JA, et al. Gene ontology: tool for the unification of biology. The Gene Ontology Consortium. *Nat Genet.* 2000;25:25–29.
35. Minoru Kanehisa SG, Kawashima Shuichi, Okuno Yasushi, Hattori Masahiro. The KEGG resource for deciphering the genome. *Nucleic Acids Res.* 2004;32:277–280.
36. Kanehisa M, Goto S, Hattori M, et al. From genomics to chemical genomics: new developments in KEGG. *Nucleic Acids Res.* 2006;34:D354–D357.
37. Tatusov Roman L, Fedorova ND, Jackson John D, et al. The COG database: an updated version includes eukaryotes. *BMC Bioinf.* 2003;4:41.
38. Li Weizhong, Jaroszewski L, Godzik Adam. Tolerating some redundancy significantly speeds up clustering of large protein databases. *Bioinformatics.* 2002;18:77–82.
39. Saier Jr MH, Reddy VS, Tamang DG, Vastermark A. The transporter classification database. *Nucleic Acids Res.* 2014;42:D251–D258.
40. Amos Bairoch RA. The SWISS-PROT protein sequence data bank and its supplement TrEMBL. *Nucleic Acids Res.* 1997;25:31–36.
41. Magrane M, UniProt C. UniProt Knowledgebase: a hub of integrated protein data. Database (Oxford). 2011; 2011: bar009.
42. Altschul Stephen F, Gish W, Miller Webb, Myers Eugene W, Lipman David J. Basic local alignment search tool. *J Mol Biol.* 1990;215:403–410.
43. Petersen TN, Brunak S, von Heijne G, Nielsen H. SignalP 4.0: discriminating signal peptides from transmembrane regions. *Nat Methods.* 2011;8:785–786.
44. Eichinger V, Nussbaumer T, Platzer A, Jehl MA, Arnold R, Rattei T. EffectiveDB–updates and novel features for a better annotation of bacterial secreted proteins and Type III, IV, VI secretion systems. *Nucleic Acids Res.* 2016;44:D669–D674.
45. Biasini M, Bienert S, Waterhouse A, et al. SWISS-MODEL: modelling protein tertiary and quaternary structure using evolutionary information. *Nucleic Acids Res.* 2014;42:W252–W258.
46. Lovell Simon C, Davis IW, Arendall W Bryan, et al. Structure validation by Calpha geometry: phi,psi and Cbeta deviation. *Proteins: Struct, Funct, Genet.* 2003;50:437–450.
47. Janssens JC, Steenackers H, Robijns S, et al. Brominated furanones inhibit biofilm formation by *Salmonella enterica* serovar Typhimurium. *Appl Environ Microbiol.* 2008;74:6639–6648.
48. Ting Ding TL, Wang Zhi, Li Jianrong. Curcumin liposomes interfere with quorum sensing system of *Aeromonas sobria* and *in silico* analysis. *Sci Rep.* 2017;7.
49. Benkert P, Tosatto SC, Schomburg Dietmar. QMEAN-a new composite scoring function for model quality assessment. *Proteins: Struct, Funct, Bioinf.* 2008;71:261.
50. McClean KH, Winson MK, Fish L, et al. Quorum sensing and *Chromobacterium violaceum*: exploitation of violacein production and inhibition for the detection of N-acylhomoserine lactones. *Microbiology.* 1997;143:3703–3711.
51. Wepf R, Beese M, Krupinska K. Reevaluation of the documentation of the technique used for the work “Combined use of confocal laser scanning microscopy and transmission electron microscopy for visualization of identical cells processed by cryotechniques”. *Protoplasma.* 2008;232:267–269.
52. Schuster K Christian, Reese I, Urlaub Eva, Gapes J Richard, Lendl Bernhard. Multidimensional information on the chemical composition of single bacterial cells by confocal Raman microspectroscopy. *Anal Chem.* 2000;72.
53. Schuster KC, Urlaub E, Gapes JR. Single-cell analysis of bacteria by Raman microscopy: spectral information on the chemical composition of cells and on the heterogeneity in a culture. *J Microbiol Methods.* 2000;42:29–38.
54. Ivleva NP, Niessner R, Panne U. Characterization and discrimination of pollen by Raman microscopy. *Anal Bioanal Chem.* 2005;381:261–267.
55. Wagner M, Ivleva NP, Haisch C, Niessner R, Horn H. Combined use of confocal laser scanning microscopy (CLSM) and Raman microscopy (RM): Investigations on EPS – Matrix. *Water Res.* 2009;43:63–76.
56. Huan Wei E, Griffiths RI, Thompson Ian P, Bailey Mark J, Whiteley Andrew S. Raman Microscopic Analysis of Single Microbial Cells. *Anal Chem.* 2004;76:4452–4458.
57. Rosch P, Harz M, Schmitt M, et al. Chemotaxonomic identification of single bacteria by micro-Raman spectroscopy: application to clean-room-relevant biological contaminations. *Appl Environ Microbiol.* 2005;71:1626–1637.
58. Harz M, Rosch P, Peschke KD, Ronneberger O, Burkhardt H, Popp J. Micro-Raman spectroscopic identification of bacterial cells of the genus Staphylococcus and dependence on their cultivation conditions. *Analyst.* 2005;130:1543–1550.
59. Gershman Mark D, Kennedy Donald J, Noble-Wang J, et al. Multistate outbreak of *Pseudomonas fluorescens* bloodstream infection after exposure to contaminated heparinized saline flush prepared by a compounding pharmacy. *Clin Infect Dis.* 2008;47:1372–1379.
60. Sarniguet Alain, Kraus J, Henkels Marcella D, Muehlchen Andrea M, Loper Joyce E. The sigma factor e affects antibiotic production and biological control activity of *Pseudomonas fluorescens* Pf-5. *Proc Natl Acad Sci USA.* 1995;92:12255–12259.
61. Benkert P, Biasini M, Schwede T. Toward the estimation of the absolute quality of individual protein structure models. *Bioinformatics.* 2011;27:343–350.
62. Hollingsworth LRt, Brown AM, Gandour RD, Bevan DR. Computational study of HIV gp120 as a target for polyanionic entry inhibitors: exploiting the V3 loop region. *PLoS One.* 2018;13:e0190658.
63. Jain AN. Surflex: fully automatic flexible molecular docking using a molecular similarity-based search engine. *J Med Chem.* 2003;46:499–511.
64. Clark Robert D, Strizhev A, Leonard Joseph M, Blake James F, Matthew James B. Consensus scoring for ligand/protein interactions. *J Mol Graphics Modell.* 2002;20:281–295.
65. Wang Renxiao, Lu Y, Wang Shaomeng. Comparative evaluation of 11 scoring functions for molecular docking. *J Med Chem.* 2003;46:2287–2303.
66. Ru W, Wang D, Xu Y, et al. Chemical constituents and bioactivities of *Panax ginseng* (C. A. Mey.). *Drug Discov Ther.* 2015;9:23–32.
67. Brühne Friedrich, Wright Elaine. *Benzyl Alcohol. Ullmann's Encyclopedia of Industrial Chemistry.* 7th ed. Wiley; 2007 pp. 7–8.
68. Saha R, Saha N, Donofrio RS, Bestervelt LL. Microbial siderophores: a mini review. *J Basic Microbiol.* 2013;53:303–317.
69. Ren D, Zuo R, Wood TK. Quorum-sensing antagonist (5Z)-4-bromo-5-(bromomethylene)-3-butyl-2(5H)-furanone influences siderophore biosynthesis in *Pseudomonas putida* and *Pseudomonas aeruginosa*. *Appl Microbiol Biotechnol.* 2004;66:689–695.
70. Dunstall George, Rowe MT, Wisdom G Brian, Kilpatrick David. Effect of quorum sensing agents on the growth kinetics of *Pseudomonas* spp. of raw milk origin. *J Dairy Res.* 2005;72:276–280.
71. Zhu J, Huang X, Zhang F, Feng L, Li J. Inhibition of quorum sensing, biofilm, and spoilage potential in *Shewanella baltica* by green tea polyphenols. *J Microbiol.* 2015;53:829–836.
72. Liu M, Wang H, Griffiths MW. Regulation of alkaline metalloprotease promoter by N-acyl homoserine lactone quorum sensing in *Pseudomonas fluorescens*. *J Appl Microbiol.* 2007;103:2174–2184.
73. Ciofu O, Tolker-Nielsen T, Jensen PO, Wang H, Hoiby N. Antimicrobial resistance, respiratory tract infections and role of biofilms in lung infections in cystic fibrosis patients. *Adv Drug Deliv Rev.* 2015;85:7–23.
74. Srey S, Jahid IK, Ha S-D. Biofilm formation in food industries: a food safety concern. *Food Control.* 2013;31:572–585.
75. Sakuragi Y, Kolter R. Quorum-sensing regulation of the biofilm matrix genes (pel) of *Pseudomonas aeruginosa*. *J Bacteriol.* 2007;189:5383–5386.
76. Sportelli MC, Tutuncu E, Picca RA, et al. Inhibiting *P. fluorescens* biofilms with fluoropolymer-embedded silver nanoparticles: an *in-situ* spectroscopic study. *Sci Rep.* 2017;7:11870.
77. Hall-Stoodley L, Costerton JW, Stoodley P. Bacterial biofilms: from the natural environment to infectious diseases. *Nat Rev Microbiol.* 2004;2:95–108.
78. Paul N, Danese LAP, Kolter Roberto. Exopolysaccharide production is required for development of *Escherichia coli* K-12 biofilm architecture. *J Bacteriol.* 2000;182:3595–3596.